Jurnal Teknokes
International: Rapid Review: Open Access Journal **Vol. 17, No. 1, March 2024, pp. 69-76** **e-ISSN 2407-8964; p-ISSN 1907-7904**

RESEARCH ARTICLE **OPEN ACCESS**

Manuscript received January 18, 2024; revised March 10, 2024; accepted March 12, 2024; date of publication March 25, 2024
Digital Object Identifier (**DOI**): https://doi.org/10.35882/teknokes.v17i1.669

How to cite: Bahrurrizki Ramadhan, Endro Yulianto, Sari Luthfiyah and Wahyu Caesarendra, "Exploring Digital Filters for Cardiac Monitoring: A Focus on Carotid Pulse and Phonocardiogram Signals", Jurnal Teknokes, Vol. 17, No. 1, pp. 69-76, March. 2024

Exploring Digital Filters for Cardiac Monitoring: A Focus on Carotid Pulse and Phonocardiogram Signals

Bahrurrizki Ramadhan[1], Endro Yulianto[1], Sari Luthfiyah[1], and Wahyu Caesarendra[2]

[1] Department of Medical Electronics Technology, Poltekkes Kemenkes Surabaya, Surabaya, Indonesia
[2] Faculty of Integrated Technologies, Universiti Brunei Darussalam, Bandar Seri Begawan, Brunei Darussalam
Corresponding author: Endro Yulianto (email: endro76@poltekkesdepkes-sby.ac.id)

ABSTRACT Heart defect early detection and correct diagnosis have become important healthcare priorities. Tools for monitoring cardiac problems are constantly being developed, with the PCG (Phonocardiogram) and Cardiac Monitor via Carotid Pulse essential for heart evaluation. Although condenser microphones embedded in electric stethoscopes have been used in past research as PCG sensors, more advancements are still required to reduce received noise. This study investigates how well a Chebyshev type-II digital filter works to reduce noise on the cardiac monitor using PCG and carotid pulse. The PCG sensor is the GY-MAX 9814 module, which is interfaced with an Arduino Uno microcontroller. Matlab, Visual Studio (used as a graph viewer), and Doppler Simulator (used as a phantom cardiac signal) are used. SNR (Signal to Noise Ratio) is used in the analysis to assess the effectiveness of two digital filter orders. The average SNR value for the Doppler Simulator is 0.001404 dB at order 2, however, it climbs dramatically to 18.60023 dB at level 4 according to the results of the SNR analysis. The average SNR value in human signals is 11.50718 dB before the filter, 0.001404 dB after the post-order 2 filter, and 12.0009 dB after the post-order 4 filter. According to the results, the digital filter of order 4 is more effective in reducing noise. This study highlights the possibility of an order 4 digital filter to improve the Cardiac Monitor through PCG and Carotid Pulse. Through enhanced signal quality, the creation of this gadget holds the potential for streamlining the identification of cardiac problems. Future developments in this technology could lead to more precise and trustworthy cardiac exams, which would help with early diagnosis and treatment of cardiovascular health.

INDEX TERMS GY-MAX 9814, Chebyshev Type II, Signal to Noise Ratio, Phonocardiogram

I. INTRODUCTION

The conventional methods of cardiac monitoring face challenges in achieving optimal accuracy and efficiency. Traditional techniques often encounter issues related to noise, interference, and the limitations of singular monitoring modalities. This necessitates innovative approaches to enhance diagnostic capabilities, reduce errors, and offer a more holistic view of cardiovascular health. Cardiac Monitor is a device to monitor the patient's heart condition to detect heart abnormalities. One method to detect early heart disease is to listen to heart sounds using a stethoscope called the auscultation technique assisted by seeing carotid pulse signals [1]. A stethoscope is positioned in the Pulmonary Artery for PCG sensor recording. The Cardiac Monitor operates by utilizing a mic condenser embedded in the stethoscope for PCG parameters, while Carotid Pulse recordings, representing carotid artery pressure signals, are obtained by leads on the neck. These results, both from Carotid Pulse and PCG signal recordings, are then displayed on a personal computer [2][3].

Several studies on signal processing in cardiac monitoring have been carried out. The journey commences with the introduction of the JM-Filter, an efficient FFT-based algorithm designed for specific frequency detection in monitored signals. This innovation is characterized by reduced iterations and enhanced signal-to-quantization noise ratio [4]. As we delve deeper, the integration of ECG and PCG monitoring systems emerges, presenting a multifaceted approach to cardiac auscultation. The incorporation of wavelet-based QRS complex detection algorithms not only augments diagnostic efficiency but also facilitates real-time monitoring through smartphone applications [5].

Moving forward, a meticulous exploration of combined ECG and SCG (Seismocardiogram) signals unfolds, showcasing the potential for continuous and non-invasive

cardiac health monitoring. The proposed mechanisms for differentiating normal and abnormal morphology, coupled with a Naïve Bayes conditional probability model, illuminate the path toward robust cardiac health assessment [6]. Concurrently, the advent of portable electrocardiograms equipped with ZigBee connectivity exemplifies a transformative leap, enabling remote observation and treatment for cardiac patients [7].

Augmented Phonocardiogram acquisition and analysis systems, designed to improve auscultation skills, offer a glimpse into the future of medical training aids. Simplicity, low cost, and diagnostic advice embedded in these systems promise accessibility, particularly in developing countries [8]. The article then explores the development of electronic stethoscopes implementing filters with operational amplifiers, fostering clarity and accuracy in cardiac and respiratory signal monitoring [9].

Filter design emerges as a pivotal theme, with a focus on digital filters essential for ECG signal processing. The article introduces practical solutions for reducing interference and baseline drift in ECG signals through the implementation of Low Pass, Band-Stop, and Zero-Phase filters [10]. Further innovations unfold in the design of a cardiac monitor for multi-parameters, encompassing ECG, PCG, and Carotid Pulse signals. The utilization of Delphi programming, instrumentation amplifiers, and Arduino microcontrollers enhances real-time monitoring capabilities [2].

Additionally, the exploration extends to the implementation of digital FIR notch filters using FPGA technology, addressing power line interference in ECG signals. This technology's parallel processing prowess, capable of 3 million operations per second, underscores its potential in real-time digital convolution algorithms [11].

Machine learning takes center stage with the classification of electrocardiograms using Self-Organizing Maps (SOM), Learning Vector Quantization (LVQ), and beat detection methods. The proposed methodologies significantly enhance arrhythmia localization and underscore the importance of smart beat detection systems [12]. In the realm of remote photoplethysmography (rPPG), optimal digital filter selection becomes paramount for accurate vital signs recognition. The comparative analysis of 100 filters on over 300 rPPG signals reveals the Chebyshev II filter with a 4th order as the optimal choice for signal preprocessing [13].

A comprehensive survey of filtering techniques applied to ECG signals provides an in-depth understanding of the performance metrics of FIR and IIR filters. The study emphasizes the importance of appropriate filter selection for denoising specific types of interference in ECG signals [14]. In the pursuit of enhancing diagnostic capabilities, the article unfolds the experimental research of digital filtering for separating breathing signals and heart contractions. The developed algorithm effectively separates breathing and heartbeat signals, paving the way for accurate vital sign assessment [15].

Entropy analysis becomes a focal point, shedding light on the impact of finite numerical resolution on digital filters. The positive correlation between filter order and Shannon entropy, coupled with the efficiency of entropy over signal-to-noise ratio, introduces a novel perspective for designing digital filters [16]. The integration of ultra-wideband radar technology presents a non-intrusive method for monitoring heart activity. The proposed method extracts heartbeat information through radar pulses, demonstrating its accuracy and potential for diagnosing heart conditions remotely [17].

As the article navigates through diverse digital filtering applications, it unravels the intricacies of cardiac signal processing [18][19]. From motion artifacts reduction in cardiac pulse signals obtained from video imaging to the development of a Heart Rate Variability analysis tool, each innovation contributes to the holistic understanding of cardiac health [20].The concluding sections delve into the design of novel three-lead electrodes for ECG and PPG data capture, envisioning a future where bulky blood pressure measurement devices are replaced by reliable and non-intrusive monitoring systems [21][22]. The integration of Vision Transformer Architecture and Hidden Semi-Markov Models in detecting heart murmurs signifies the pivotal role of artificial intelligence in augmenting diagnostic accuracy [23].

The article culminates in the exploration of noise-affected ECG signals, introducing a pioneering solution that combines digital filters with cognitive radio technology. This innovative approach not only reduces noise but also facilitates the transmission and reception of ECG signals for precise diagnosis[24][25][26].

This research aims to explore the transformative potential of Chebyshev Type-II digital filters in cardiac monitoring, with a special focus on integrating Carotid Pulse and PCG signals. The main goal is to increase diagnostic accuracy, improve signal quality, and contribute to the development of non-intrusive and efficient cardiac monitoring systems. The article contributes a comprehensive survey of cutting-edge technologies and methodologies in cardiac monitoring, emphasizing the role of digital filters in addressing existing challenges.

II. MATERIALS AND METHOD

The following are the materials and methods needed in this research:

A. DATA COLLECTION

The author will conduct sensor testing and data collection with the aim of knowing the capabilities of the tool that has been designed.

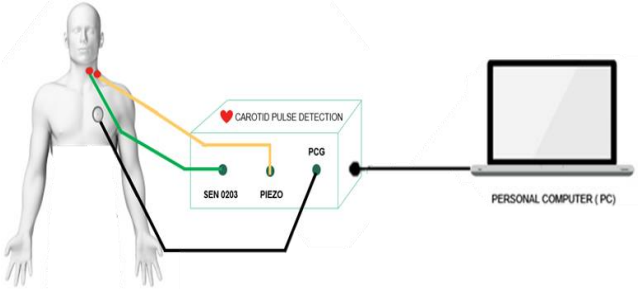

FIGURE 1. Mechanical diagram of laying parameters on a designed tool

In sensor testing, the GY-MAX 9814 sensor uses an oscilloscope to test sensor performance. Digital filter testing is carried out

with a function generator by providing a voltage of 5V as much as 22 frequency points with a frequency range of 10-300 Hz. The results of testing the function generator are quite good at passing the bandpass frequency, but the farther away from the cut-off frequency there is a non-linear frequency spike.

Module testing of doppler simulators with an average BPM value result is 59 with a setting of 60 BPM, an average BPM value result is 120.8 with a setting of 120 BPM, and an average BPM value result is 179.2 with a setting of 180 BPM. Testing of Chebyshev type II Bandpass 2nd and 4th order Infinite Impulse Response digital filters was carried out with a doppler simulator. The results obtained are in the form of SNR (Signal to Noise Ratio) values, namely for order 2 the average SNR value is 0.002619 dB and for order 4 the average SNR value is 18.60023 dB. Testing of Infinite Impulse Response Bandpass Chebyshev type II order 2 and order 4 digital filters was carried out on humans. The results obtained are in the form of SNR (Signal to Noise Ratio) values, namely for before the filter of 11.50718 dB, for order 2 SNR values of 0.001404 dB, and for order 4 SNR values of 12.0009 dB.

Based on the results of the research mentioned above, the author states that the GY-MAX 9814 sensor can be used to detect heart sound signals. In the Chebyshev type II Infinite Impulse Response Bandpass digital filter, it can be concluded that order 4 is more effective with a higher SNR value compared to order 2.

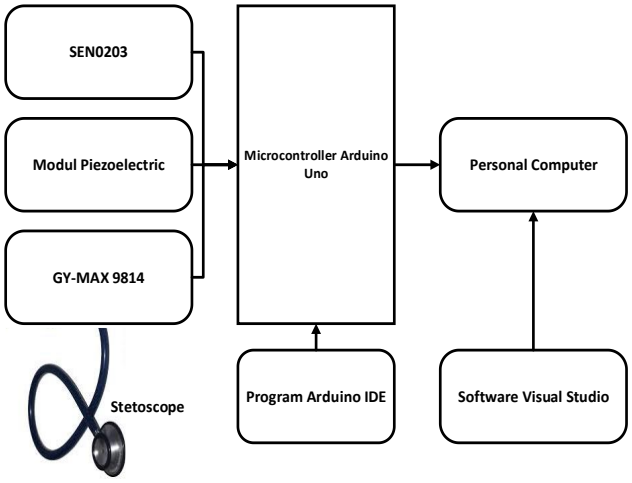

FIGURE 2. Tool System Block Diagram, using an Arduino microcontroller and display using a Personal Computer

FIGURE 2 shows a block diagram of the entire system. The output of the Piezoelectric, SEN0203, and GY-MAX 9814 sensor modules will be processed on a microcontroller program that will enter the Arduino analog pin which will process from analog data to digital data. Digital data from Arduino will be received by Personal Computer via USB cable which then the data will be processed using Visual Studio software. Processing in Visual Studio is used to display PCG and Carotid Pulse in real time.

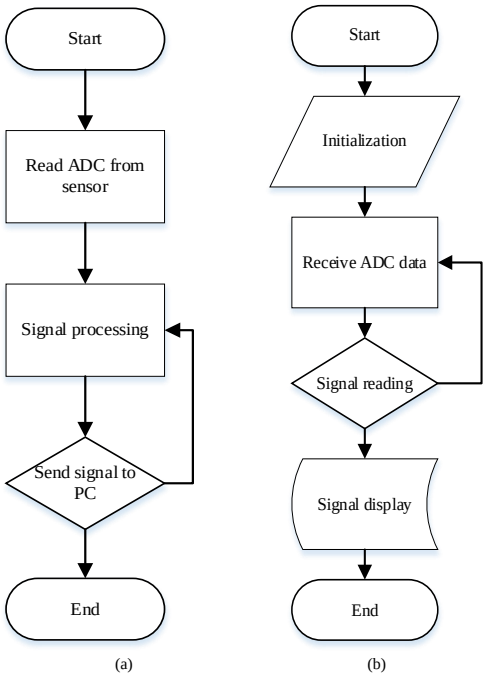

FIGURE 3. Flowchart Arduino (a) and Flowchart Visual Studio (b)

FIGURE 3 displays two images, namely (a) Arduino flow diagram, (b) Visual Studio flow diagram on PC. For (a) When the device is activated it will initiate the initialization of ADC data from the carotid sensor consisting of piezoelectricity and SEN0203 detect carotid signal, from the GY-MAX 9814 sensor used to detect heart sound signals on the *Phonocardiogram*. After initialization is complete, the program will read the ADC data to be processed to the microcontroller. In microcontrollers, the process of converting analog signals to digital data occurs so that they can be processed. Once read, the program will provide a code sending carotid signals and heart sound signals *to the Personal Computer via a USB cable to be received on the* Personal Computer. Whereas (b) when the microcontroller sends data, it will command the program on the PC to perform the initial initialization. After the initial initialization is done, the next process is to receive ADC data by encoding data so that it can be distinguished for the processing process, if "NO" then the program will return to the ADC data receiving process, if "YES" then the data will be processed in the Visual Studio program to be displayed in *real time* and simultaneously. On the graphic display, the program will start displaying the *Carotid Pulse* and *Phonocardiogram*.

B. DATA ANALYSIS

SNR (Signal to Noise Ratio) is a measure used in signal analysis to compare the desired signal level with the background noise level or is defined as the ratio of signal strength to noise strength. If a signal contains Gaussian White Noise $n(t)$, the contaminated signal $x_1(t)$ can be explained using the following Equation (1) [27].

$$x_1(t) = x(t) + n(t) \quad (1)$$

The SNR value can be calculated using a formula that relates signal strength to noise, shown in Equation (2) [27]and if expressed in decibels (dB), shown in Equation (3) [28] [29] [30].

$$SNR = \frac{\sum_{t=0}^{L-1} x^2(t)}{\sum_{t=0}^{L-1} n^2(t)} \quad (2)$$

$$SNR = 10log_{10}\frac{P_s}{P_n} \quad (3)$$

Where in Equation (2), the L is the length of the signal and in Equation (3), the P_s and P_n value is a power signal and noise signal produced from a signal.

C. RESULT

After the signal acquisition device consisting of sensors, signal processing and output has been completed, several tests are carrid out. Initial testing is performed to ensure that each part of the signal acquisition device is functioning properly.

FIGURE 5. Device modul

FIGURE 5 shows a tool module consisting of a stethoscope connected to a GY-MAX 9814 sensor, a biomechanical sensor that is piezoelectric, and a biooptical sensor SEN0203. Each is connected to an Arduino uno microcontroller. In this researh, the oscilloscope has tested the sensor, namely GY-MAX 9814 so that the sensor is stated to work as expected. Function generators are used for filter testing, and data retrieval using doppler simulators and humans so that the following results are found.

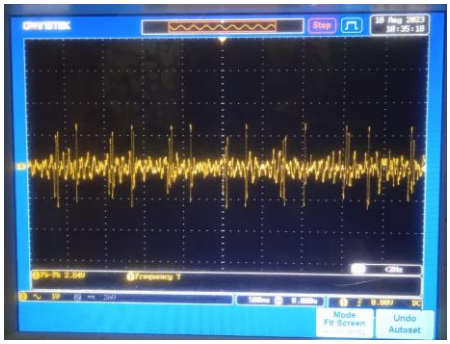

FIGURE 6. GY-MAX 9814 output readings on oscilloscopes

FIGURE 6 shows the results of measuring the output of the GY-MAX 9814 sensor on an oscilloscope with settings of 1 Volt/DIV and Time/DIV of 500 mS. The amplitude of the sensor output reads 2.64 Vpp.

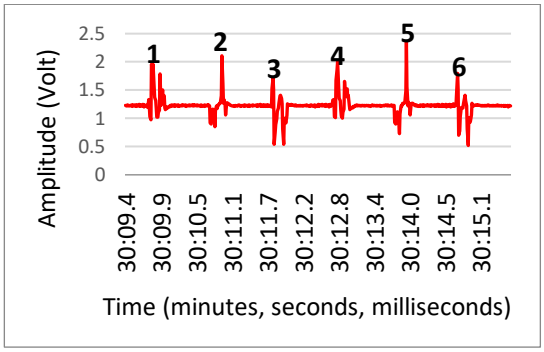

FIGURE 7. GY-MAX 9814 output readout against doppler simulator setting 60 bpm

FIGURE 7 shows the results of measurements of the doppler simulator carried out by placing the stethoscope membrane to the surface of the doppler simulator then setting bpm 60, 120, and 180 on the doppler simulator. Data retrieval using data streamer in Microsoft excel with interval settings of 10 ms and lots of data 500. Data collection has been carried out 10 times and analyzed the results of data collection in the form of the average obtained.

TABLE 1
The results of the bpm reading of the device against the doppler simulator

Signal Doppler Simulator	
Setting BPM	**BPM Readable Average**
60	59
120	120.8
180	179.2

TABLE 1 is the result of data collection which aims to compare the results of the doppler simulator setting with the readings on the module using the GY-MAX 9814 sensor.

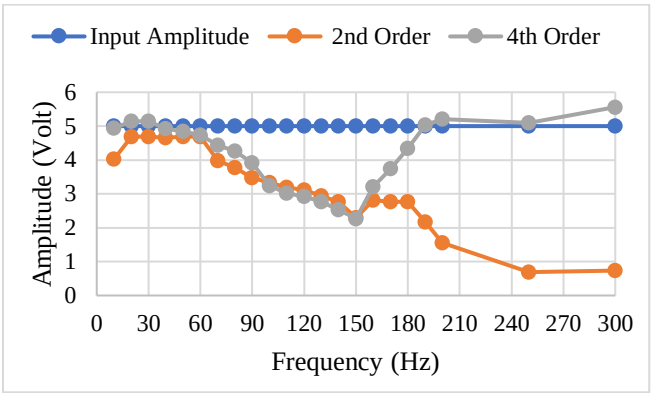

FIGURE 8. Plot graph of filter measurement against function generator

FIGURE 8 shows the results of digital filter measurements of function generators by providing an amplitude of 5 volts with a frequency range of 10-300 Hz. The results of measuring these frequency points through Chebyshev Filter type II Order 2 and Order 4. Data retrieval using a data streamer in Microsoft excel with an interval setting of 10 ms and a lot of 500 data taken the highest peak.

TABLE 2
DIgital Chebyshev Filter tipe II Measurement

Frequency (Hz)	Input Amplitude (volt)	Amplitude after filtered 2nd order Bandpass (volt)	Amplitude after filtered 4th order Bandpass (volt)
10	5	4,02	4,94
20	5	4,69	5,15
30	5	4,69	5,15
40	5	4,66	4,92
50	5	4,69	4,84
60	5	4,69	4,73
70	5	3,98	4,43
80	5	3,77	4,26
90	5	3,47	3,92
100	5	3,33	3,24
110	5	3,19	3,01
120	5	3,12	2,92
130	5	2,94	2,77
140	5	2,77	2,53
150	5	2,3	2,27
160	5	2,82	3,21
170	5	2,77	3,74
180	5	2,77	4,34
190	5	2,17	5,03
200	5	1,55	5,21
250	5	0,69	5,1
300	5	0,73	5,56

TABLE 2 is the result of measurements of 22 frequency points on the Chebyshev Bandpass filter type II with frequency points ranging from 10-300 Hz with ampitudes at each frequency of 5 Volts. The measurement results of these frequency points were passed to the Chebyshev Bandpass Filter type II with different order values, namely, Chebyshev Bandpass Filter type II with order 2 and Chebyshev Bandpass Filter type II with order 4.

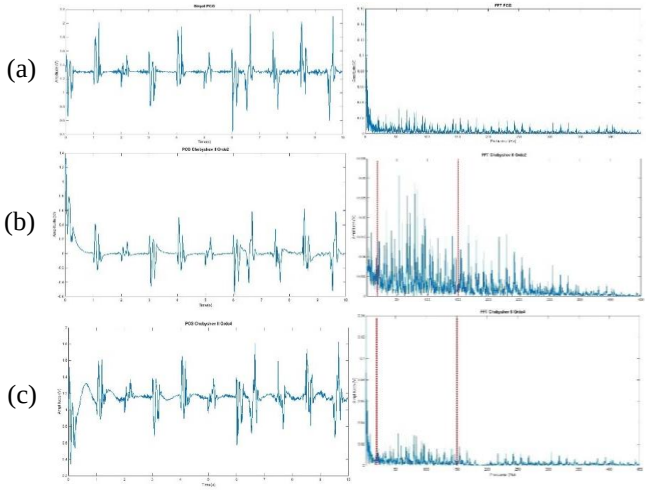

FIGURE 9. Signal graphic and FFT doppler simulator (a), filter chebyshev orde 2 (b), filter chebyshev orde 4 (c).

FIGURE 9 shows the signal and FFT results from the doppler simulator input (a), signal and FFT after passing through the Chebyshev type II digital filter order 2 (b), and the signal and FFT after passing through the Chebyshev type II digital filter order 4 (c).

TABLE 3
Results SNR Filter DIgital Chebyshev Type II

Signal Doppler Simulator	SNR value Bandpass Chebyshev orde 2 (dB)	SNR value Bandpass Chebyshev orde 4 (dB)
1	0.002643	18.682395
2	0.002572	18.608270
3	0.002557	18.600949
4	0.002564	18.541718
5	0.002619	18.630654
6	0.002669	18.462214
7	0.002619	18.630654
8	0.003032	18.598799
9	0.002192	18.500611
10	0.002723	18.746079
Average	**0.002619**	**18.60023**

TABLE 3 is the SNR result of the simulator doppler signal after passing through Chebyshev type II digital filters of order 2 and order 4.

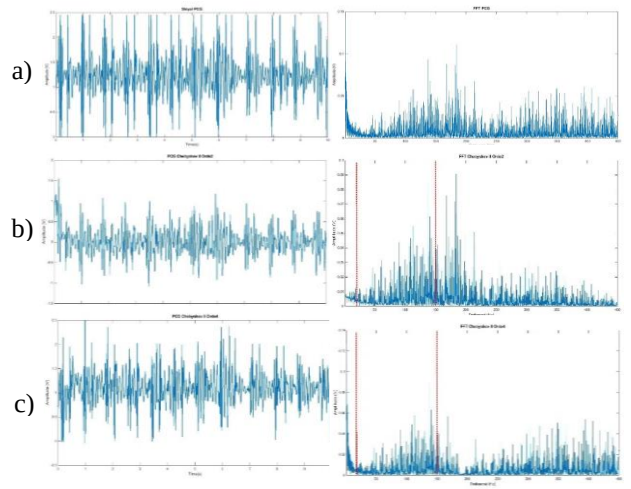

FIGURE 10. Signal charts and FFT Human respondents (a), filter chebyshev orde 2 (b), filter chebyshev orde 4 (c).

FIGURE 10 shows the results of the signal and FFT from human respondent input (a), signal and FFT after passing through the Chebyshev type II digital filter order 2 (b), and the signal and FFT after passing through the Chebyshev type II digital filter order 4 (c).

TABLE 4
Results SNR Filter DIgital Chebyshev Type II

Data Responden	Signal SNR Value Input (dB)	Signal SNR Value Bandpass Chebyshev orde 2 (dB)	Signal SNR Value Bandpass Chebyshev orde 4 (dB)
1	9.578454	0.000547	10.341091
2	10.013111	0.000979	10.439982
3	12.138479	0.001678	12.607597
4	15.39048	0.002951	15.856289
5	9.198046	0.00106	9.559617
6	12.724484	0.001207	13.200812
Average	**11.50718**	**0.001404**	**12.0009**

TABLE 3 is the SNR result of the simulator doppler signal after passing through Chebyshev type II digital filters of order 2 and order 4.

D. DISCUSSION

This discussion section explains the research results in the form of hardware and software for data acquisition purposes through carotid sensors consisting of piezoelectric and SEN0203 which detect carotid signals, and PCG sensors namely GY-MAX 9814 which detect heart sound signals. The signal obtained was then subjected to a series of tests with Chebyshev type-II digital filters to obtain a signal that was clean from noise. The discussion section consists of four subsections, namely interpretation of the results, comparison with other related research, weaknesses or limitations of this research, and implications of this research.

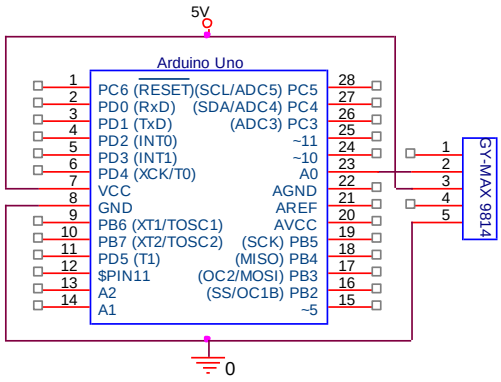

FIGURE 11. Diagram Schematics GY-MAX 9814 and Arduino Uno

FIGURE 11 is a series of GY-MAX 9814 sensors on the Arduino Uno microcontroller board. This GY-MAX 9814 sensor requires a voltage of 2.7-5.5 Volts connected to the Arduino Uno Vin pin, and the GND pin is connected to the Arduino Uno ground pin. The output pin is connected to the analog pin A0 on the Arduino Uno. Here is the program Arduino filter Chebyshev type II:

```
// Koefisien Filter Chebyshev orde 4
const float b[5] = {0.76410706970357423, -
2.0854887215653983, 2.6513445413572043 , -
2.0854887215653983, 0.76410706970357423};
const float a[5] = {1.0, -2.6552004353181986,
3.0256662288390066, -2.0247132283517777,
0.66387574181657028};

void loop() {
int pcgValue = analogRead(pcgPin);
  float pcgVoltage = pcgValue * (5.0 / 1023.0);
// konversi adc ke tegangan

// Filter Chebyshev orde 4 untuk PCG
const float pcg_chebyshevFilteredValue =
chebyshevFilter(pcgVoltage, b, a)*0.1;}

float chebyshevFilter(float inputValue, const
float b[5], const float a[5]) {

  static float prevSamples[5] = {0};

  float outputValue = b[0] * inputValue + b[1]
* prevSamples[0] + b[2] * prevSamples[1] + b[3]
* prevSamples[2] + b[4] * prevSamples[3]
                  - a[1] * prevSamples[1] -
a[2] * prevSamples[2] - a[3] *
prevSamples[3] - a[4] * prevSamples[4];

  prevSamples[4] = prevSamples[3];
  prevSamples[3] = prevSamples[2];
  prevSamples[2] = prevSamples[1];
  prevSamples[1] = prevSamples[0];
  prevSamples[0] = inputValue;

  return outputValue;
}
```

The graphical display of Visual Studio on a PC is shown in FIGURE 12. When the start button on the initial display is pressed, with the description carotid1(purple) is a graph of the piezoelectric sensor, carotid2(red) is a graph of the SEN0203 sensor, PCG1(blue) is a graph of the GY-MAX 9814 sensor before the filter, and PCG2 (dark yellow) is a graph of the GY-MAX 9814 sensor after filtering.

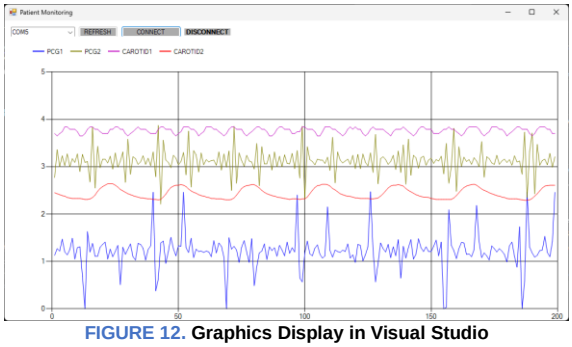

FIGURE 12. Graphics Display in Visual Studio

The overall system performance begins when the device is activated, then the device initiates the initialization of ADC data from carotid sensors consisting of piezoelectricity and SEN0203 that detect carotid signals, and PCG (Phonocardiogram) sensors, namely GY-MAX 9814 that detect heart sound signals. After initialization is complete, the program will read the ADC data to be processed to the microcontroller. In microcontrollers, there is a process of converting analog signals from reading ADC data to digital data so that it can be processed. For heart sound signals are processed again with Chebyshev type-II digital filters. Upon completion of the ADC reading and the program filter will provide a code sending carotid signals and heart sound signals to the Personal Computer via a USB cable to be received on the Visual Studio Code program to be displayed in real time and simultaneously.

In this research several measurements and tests were carried out. Measurement of GY-MAX9814 output using an oscilloscope, the signal reads at 2.64 Vpp. Filter testing using function generators found in FIGURE 7 and TABLE 2. Data retrieval using doppler simulator with BPM setting 60 reading an average of 59, setting 120 reading an average of 120.8 and setting 180 reading an average of 179.2. SNR analysis on Chebyshev type II digital filter against doppler simulator with average results of 0.002619 dB for order 2 and 18.60023 dB for order 4. SNR analysis of Chebyshev type II digital filter on human respondents with results of 0.001404 dB for order 2 and 12.0009 dB for order 4.

Research [31] carried out PCG signal denoising using Discrete Wavelet Transform (DWT) by selecting several types of Mother Wavelet (MWT) by the Decomposition Level (DL) function and various threshold types. In this study, the sym20 wavelet type with 10 decomposition levels and Bayesian Soft Thresholding function provided the best results in denoising the applied PCG signals with an SNR value of 20.1290. The research [32] also carried out denoising of the PCG signal using DWT. The results showed that Symlet DL 5 gave slightly better results compared to Daubechies DL 5 with values of 16.1686 and 16.1634

The limitation of this research lies in the acquisition device to obtain PCG signals using a condenser mic which captures sound from the stethoscope so that the noise produced is more compared to a piezo electric sensor which is more focused on capturing heart sounds.

The integration of digital filters in cardiac monitoring has the potential to enhance diagnostic precision by reducing noise, interference, and signal distortions. This could lead to more accurate diagnosis of cardiac abnormalities and conditions, enabling healthcare providers to deliver more targeted and effective treatments.

III. CONCLUSION

The aims of this article is to explore the transformative potential of Chebyshev Type-II digital filters in cardiac monitoring. this research successfully validates the GY-MAX 9814 sensor's proficiency in detecting heart sound signals, both in simulated conditions and real human subjects, emphasizing its potential for reliable cardiac monitoring. The Visual Studio software demonstrated effective signal display capabilities for carotid signals and phonocardiograms. The results of the SNR value obtained from the Doppler Simulator heart sound signal after digital filtering showed an effective SNR value found in the Chebyshev Bandpass type-II digital filter with order 4 with an average SNR value of 18.60023 dB, compared to order 2 which had an average SNR value of 0.002619 dB. The SNR value obtained from the sound signal of the human heart after an effective filter are found in order 4 of the average SNR value of 11.50718 dB rose to 12.0009 dB, while in order 4 experienced a decrease in SNR value to 0.001404 dB. Future work should focus on algorithm optimization, extended clinical trials for diverse patient populations, real-time monitoring implementation, exploration of additional filter types, and integration of wireless transmission for remote monitoring, collectively enhancing the overall efficacy and practicality of cardiac monitoring systems in diverse healthcare settings.

REFERENCE

[1] M. N. Manjunatha, M. Venukumar, E. Raghavendra, M. Varsha, R. Sandeep, and A. A. Audre, "ECG and PPG Data Capture using Novel Three Lead Electrode," *Int. Conf. Curr. Trends Comput. Electr. Electron. Commun. CTCEEC 2017*, pp. 495–498, 2018, doi: 10.1109/CTCEEC.2017.8455176.

[2] R. Alvionita *et al.*, "Design of Cardiac Monitor for Multi Parameters," *Proc. - 2019 Int. Semin. Appl. Technol. Inf. Commun. Ind. 4.0 Retrosp. Prospect. Challenges, iSemantic 2019*, no. February 2020, pp. 423–428, 2019, doi: 10.1109/ISEMANTIC.2019.8884264.

[3] W. Caesarendra, T. Triwiyanto, H. G. Ariswati, A. R. Masnulula, and N. M. Firdaus, "Development of Cardiac Monitor Through Carotid Pulse, Phonocardiography and Electrocardiography," *J. Teknokes*, vol. 15, no. 2, pp. 81–87, Jun. 2022, doi: 10.35882/JTEKNOKES.V15I2.132.

[4] M. A. Jaber and D. Massicotte, "The JM-Filter to Detect Specific Frequency in Monitored Signal," *IEEE Trans. Signal Process.*, vol. 69, pp. 1468–1476, 2021, doi: 10.1109/TSP.2021.3053509.

[5] S. Y. Lee, P. W. Huang, J. R. Chiou, C. Tsou, Y. Y. Liao, and J. Y. Chen, "Electrocardiogram and Phonocardiogram Monitoring System for Cardiac Auscultation," *IEEE Trans. Biomed. Circuits Syst.*, vol. 13, no. 6, pp. 1471–1482, 2019, doi: 10.1109/TBCAS.2019.2947694.

[6] P. K. Sahoo, H. K. Thakkar, W. Y. Lin, P. C. Chang, and M. Y. Lee, "On the Design of an Efficient Cardiac Health Monitoring System Through

Combined Analysis of ECG and SCG Signals," *Sensors*, vol. 18, no. 2, Feb. 2018, doi: 10.3390/S18020379.
[7] M. Ehnesh, P. Abatis, and F. S. Schlindwein, "A portable electrocardiogram for real-time monitoring of cardiac signals," *SN Appl. Sci.*, vol. 2, no. 8, Aug. 2020, doi: 10.1007/S42452-020-3065-9.
[8] N. E. Reed and T. R. Reed, "Augmented phonocardiogram acquisition and analysis," *Lect. Notes Comput. Sci. (including Subser. Lect. Notes Artif. Intell. Lect. Notes Bioinformatics)*, vol. 6780 LNAI, pp. 618–627, 2011, doi: 10.1007/978-3-642-21852-1_71/COVER.
[9] E. A. GONZÁLEZ-GALINDO, F. J. RÍOS-MENDOZA, J. K. CASTRO-PÉREZ, and F. J. DOMÍNGUEZ-ROMERO, "Development of an electronic stethoscope implementing filters with OPAM for the observation of cardiac signals using a graphical interface with an AD8232 module," *Rev. Ing. Eléctrica*, pp. 1–14, Aug. 2023, doi: 10.35429/JEE.2023.19.7.1.14.
[10] "Filter design for ECG signal processing," *Int. J. Front. Eng. Technol.*, vol. 4, no. 5, 2022, doi: 10.25236/IJFET.2022.040508.
[11] D. K. Aboutabikh, D. I. Haidar, and D. N. Aboukerdah, "Design and implementation of a digital FIR notch filter for the ECG signals using FPGA," *Ijarcce*, vol. 5, no. 1, pp. 452–456, Jan. 2016, doi: 10.17148/IJARCCE.2016.51112.
[12] M. H. Baig, A. Rasool, and M. I. Bhatti, "Classification of electrocardiogram using SOM, LVQ and beat detection methods in localization of cardiac arrhythmias," *2001 Conf. Proc. 23rd Annu. Int. Conf. IEEE Eng. Med. Biol. Soc.*, vol. 2, pp. 1684–1687, 2001, doi: 10.1109/IEMBS.2001.1020539.
[13] S. Guler, A. Golparvar, O. Ozturk, H. Dogan, and M. Kaya Yapici, "Optimal digital filter selection for remote photoplethysmography (rPPG) signal conditioning," *Biomed. Phys. &Amp; Eng. Express*, vol. 9, no. 2, Mar. 2023, doi: 10.1088/2057-1976/ACAF8A.
[14] "Survey on Filtering Techniques Applied to ECG Signal," *Int. J. Innov. Technol. Explor. Eng.*, vol. 9, no. 7S, pp. 9–11, May 2020, doi: 10.35940/IJITEE.G1003.0597S20.
[15] M. Nosach, "Experimental research of digital filtering in the separation of breathing signals and heart contractions to assess the control of the driver's condition," *J. Für Mobilität Und Verkehr*, no. 4, pp. 45–51, Nov. 2019, doi: 10.34647/JMV.NR4.ID32.
[16] V. S. Borges, E. G. Nepomuceno, C. A. Duque, and D. N. Butusov, "Some Remarks about Entropy of Digital Filtered Signals," *Entropy*, vol. 22, no. 3, Mar. 2020, doi: 10.3390/E22030365.
[17] H. S. Cho, B. Choi, and Y. J. Park, "Monitoring heart activity using ultra-wideband radar," *Electron. Lett.*, vol. 55, no. 16, pp. 878–881, Aug. 2019, doi: 10.1049/EL.2019.1438.
[18] D. N. Purnamasari, K. A. Wibisono, and H. Sukri, "Digital Moving Average Filter Application for Echo Signals and Temperature," *E3S Web Conf.*, vol. 328, Dec. 2021, doi: 10.1051/E3SCONF/202132802007.
[19] V. M. Shervegar, "Phonocardiogram event-based delineation method using continuous wavelet transform," *Int. J. Health Sci. (Qassim).*, pp. 4039–4054, Jun. 2022, doi: 10.53730/IJHS.V6NS4.9032.
[20] M. Al-Yoonus, M. H. Alhabib, M. Z. Nayef Al-Dabagh, and M. F. L. Abdullah, "Motion artifacts reduction in cardiac pulse signal acquired from video imaging," *Int. J. Electr. Comput. Eng.*, vol. 10, no. 6, p. 5687, Dec. 2020, doi: 10.11591/ijece.v10i6.pp5687-5693.
[21] J. M. Medeiros, "Development of a Heart Rate Variability analysis tool," 2010, [Online]. Available: http://citeseerx.ist.psu.edu/viewdoc/download?doi=10.1.1.460.2891&rep=rep1&type=pdf.
[22] J. Kim, G. Park, and B. Suh, "Classification of Phonocardiogram Recordings using Vision Transformer Architecture," *Comput. Cardiol. Conf.*, vol. 2022-September, 2022, doi: 10.22489/CINC.2022.084.
[23] A. McDonald, M. J. F. Gales, and A. Agarwal, "Detection of Heart Murmurs in Phonocardiograms with Parallel Hidden Semi-Markov Models," *Comput. Cardiol. Conf.*, vol. 2022-September, 2022, doi: 10.22489/CINC.2022.020.
[24] X. Wei, B. Yin, and Z. Zhu, "Noise Filtering Design of Non-intrusive Electrical Monitoring System," *Proc. 2016 4th Int. Conf. Mach. Mater. Inf. Technol. Appl.*, 2016, doi: 10.2991/ICMMITA-16.2016.292.
[25] Z. Wang, B. Jin, S. Li, F. Zhang, and W. Zhang, "ECG-grained Cardiac Monitoring Using UWB Signals," *Proc. ACM Interactive, Mobile, Wearable Ubiquitous Technol.*, vol. 6, no. 4, Jan. 2023, doi: 10.1145/3569503.
[26] M. Premkumar, S. Sathiyapriya, M. Arun, and V. Sachan, "Medical Signal Processing via Digital Filter and Transmission Reception Using Cognitive Radio Technology," *Trait. Du Signal*, vol. 39, no. 4, pp. 1357–1362, Aug. 2022, doi: 10.18280/TS.390429.
[27] A. Marjaninejad, F. Almasganj, and A. J. Sheikhzadeh, "Online signal to noise ratio improvement of ECG signal based on EEMD of synchronized ECG beats," *2014 21st Iran. Conf. Biomed. Eng. ICBME 2014*, pp. 113–118, Feb. 2011, doi: 10.1109/ICBME.2014.7043904.
[28] F. L. Mvuh, C. O. V. Ebode Ko'a, and B. Bodo, "Multichannel high noise level ECG denoising based on adversarial deep learning," *Sci. Reports 2023 141*, vol. 14, no. 1, pp. 1–13, Jan. 2024, doi: 10.1038/s41598-023-50334-7.
[29] Y. Zhang, S. Wei, C. Di Maria, and C. Liu, "Using Lempel–Ziv Complexity to Assess ECG Signal Quality," *J. Med. Biol. Eng.*, vol. 36, no. 5, p. 625, Oct. 2016, doi: 10.1007/S40846-016-0165-5.
[30] M. Welvaert and Y. Rosseel, "On the Definition of Signal-To-Noise Ratio and Contrast-To-Noise Ratio for fMRI Data," *PLoS One*, vol. 8, no. 11, Nov. 2013, doi: 10.1371/JOURNAL.PONE.0077089.
[31] R. M. P. Et. al., "Optimal Parameter Selection for DWT based PCG Denoising," *Turkish J. Comput. Math. Educ.*, vol. 12, no. 10, pp. 7521–7532, Apr. 2021, doi: 10.17762/TURCOMAT.V12I10.5658.
[32] M. Rouis, A. Ouafi, and S. Sbaa, "Optimal level and order detection in wavelet decomposition for PCG signal denoising," *Biomed. Tech.*, vol. 64, no. 2, pp. 163–176, Apr. 2019, doi: 10.1515/BMT-2018-0001/MACHINEREADABLECITATION/RIS.